広島大学学位請求論文

Reexamination of the immunological rejection model on tail regression during anuran metamorphosis

(無尾両生類の変態での尾部退縮に関する拒絶反応説の再検討)

２０１６年

広島大学大学院理学研究科

生物科学専攻

中井　裕也

目　次

主論文

Reexamination of the immunological rejection model on tail regression during anuran metamorphosis

Yuya Nakai

Department of Biological Science,
Graduate School of Science,
Hiroshima University

Contents

Abstract

Tail regression is one of the most prominent transformations observed during anuran metamorphosis. A tadpole tail that is twice as long as the tadpole trunk nearly disappears within three days in *Xenopus tropicalis*. Several years ago, it was proposed that this phenomenon is driven by an immunological rejection of larval-skin-specific antigens, Ouro proteins. We generated *ouro*-knockout tadpoles using the TALEN method to reexamine this immunological rejection model. Both the *ouro1*- and *ouro2*-knockout tadpoles expressed a very low level of mRNA transcribed from a targeted *ouro* gene, an undetectable level of Ouro protein encoded by a target gene and a scarcely detectable level of the other Ouro protein from the untargeted *ouro* gene in tail skin. Furthermore, congenital athymic frogs were produced by *Foxn1* gene modification. Flow cytometry analysis revealed that mutant frogs lacked splenic $CD8^+$ T cells, which play a major role in cytotoxic reaction. Furthermore, T cell-dependent skin allograft rejection was dramatically impaired in mutant frogs. None of the knockout tadpoles showed any significant delay in the process of tail shortening during the climax of metamorphosis, which demonstrates that Ouro proteins are not essential to tail regression at least in *Xenopus tropicalis* and argues against the immunological rejection model.

Introduction

Anuran metamorphosis has been a highly studied phenomenon for more than a century (Hertwig 1898). This process involves a systematic and physiological change from a larva to an adult, including the resorption of larval organs, development of adult organs, and remodeling of many organs and tissues. Tail regression is an especially conspicuous and dynamic change (Nakajima *et al.* 2005).

Thyroid hormone (TH) involvement in tadpole tail regression has been substantiated by the report that isolated tadpole tail tips shrink in the presence of thyroxine (Weber 1962). This TH-dependent tail resorption is also supported by the finding that metamorphic morphological changes, including the tail shortening program, are inhibited in transgenic *Xenopus laevis* (*X. laevis*) tadpoles overexpressing type III deiodinase, which degrades TH (Huang *et al.* 1999). A cultured myoblastic cell line derived from *X. laevis* tadpole tail died by apoptosis in response to TH (Yaoita & Nakajima 1997). In this process, a paracrine mechanism based on a TH-dependent soluble death-inducing factor is unlikely because cell death is not facilitated by adding the conditioned medium when cells were cultured with TH, suggesting a cell-autonomous manner, namely, the suicide model. This type of cell death of tail muscle in the presence of TH is observed during the climax of metamorphosis (stage 58-66), when many orchestrated changes appear simultaneously, and is almost completely inhibited by the overexpression of dominant-negative TH receptor (DNTR)

(Das *et al.* 2002; Nakajima & Yaoita 2003).

Another mechanism that has been proposed suggests that programmed cell death is induced in a tail through the loss of a cell's attachment to the extracellular matrix (ECM) due to the TH-dependent expression of ECM-degrading proteases such as collagenase-3 and stromelysin-3 (Brown *et al.* 1996) in the subepidermal fibroblasts surrounding the muscle cells, which is called the murder model (Berry *et al.* 1998). When a portion of the tail muscle cells are transfected with *DNTR*, non-transfected muscle cells that surround *DNTR*-expressing cells secrete ECM-degrading enzymes in response to TH to break down the ECM, and even *DNTR*-expressing cells are murdered (Fujimoto *et al.* 2007; Nakajima & Yaoita 2003). Cell death by murder starts at stage 62, when TH reaches a peak, and the expression of many types of ECM-degrading enzymes begin to show a prominent rise, especially MMP-9TH (Fujimoto *et al.* 2006).

The immunological rejection of a tail has been proposed as a third model. This idea originally comes from the findings that young frogs reject skin grafts from syngenic tadpole tails and that the secondary response of rejection is accelerated (Izutsu & Yoshizato 1993). This model is becoming generally accepted because precocious tail degeneration is promoted by the overexpression of *ouro1* and *ouro2*, which encode keratin-related proteins and are specifically expressed in larval skin, and because the knockdown of one *ouro* gene slows down the tail regression process and results in tailed frogs (Mukaigasa *et al.* 2009).

In the immunological rejection model, a tailed frog is produced by the knockdown of *ouro* gene expression (Mukaigasa *et al.* 2009). As TH treatment represses

Ouro protein expression in the tail (Watanabe *et al.* 2003), it should impair the immunological rejection of Ouro proteins. In contrast, tailed frogs are also generated by reducing TH signaling during the climax through methimazole treatment of stage 57/58 tadpoles to inhibit TH synthesis (Elinson *et al.* 1999) or through overexpression of type III deiodinase to inactivate TH (Huang *et al.* 1999).

In this study, we reexamine the immunological rejection model. Using targeted gene disruption, which has become a common and facile method, *ouro1*- and *ouro2*-knockout tadpoles were generated using the TALEN method, and congenital athymic tadpoles were created by modifying the *Foxn1* gene to delete T cells. Tail regression was examined and compared with wild-type tadpoles.

Experimental Procedures

Animals

The Ivory Coast and Nigerian H (Yasuda) lines of *X. tropicalis* were provided by the Institute for Amphibian Biology (Graduate School of Science, Hiroshima University) through the National Bio-Resource Project of the MEXT, Japan. Tadpoles were staged according to the Nieukoop and Faber method (Nieuwkoop & Faber 1956). Tadpoles and frogs were maintained at 26-28°C and 24°C, respectively. All of the animals were maintained and used in accordance with the guidelines established by Hiroshima University for the care and use of experimental animals.

qPCR

Total RNA was purified from tadpole skin and skinned tails using the SV Total RNA Isolation System kit (Promega), which includes a DNase I treatment step. Samples of 1 μg of total RNA were denatured at 65°C for 5 min, reverse transcribed with 9-mer random and oligo-dT primers using the ReverTra Ace qPCR RT Master Mix (TOYOBO) at 37°C for 15 min, and inactivated at 98°C for 5 min. Diluted products (2 μl) were subjected to qPCR using a SYBR Premix Ex Taq kit (TaKaRa) in 20 μl of reaction solution. qPCR was performed using a Thermal Cycler Dice Real-Time System (TaKaRa) according to the manufacturer's protocol. The reaction conditions included pre-denaturation (95°C, 30 s) and a two-step protocol [(95°C, 5 s; 60°C, 30 s) x 40].

The results were analyzed using a Thermal Cycler Dice Real-Time System Ver. 4.00 (TaKaRa). The level of specific mRNA was quantified and normalized to the level of *elongation factor 1-α* mRNA. The primer sequences used for the amplifications are shown in Table 1.

Construction of the TALENs

TALEN repeats were assembled as previously described (Cermak *et al.* 2011), with minor modifications (Nakajima *et al.* 2013), and were inserted into pTALEN-ELD and pTALEN-KKR (Lei *et al.* 2012; Nakajima & Yaoita 2013) to generate anti-*ouro1*, *anti-ouro2*, and *anti-Foxn1* TALEN expression constructs. The target sequences of TALEN are shown in Figs. 1,6,8 and 10.

RNA microinjection into fertilized eggs

mRNA was transcribed *in vitro* from the NotI-digested anti-*ouro1*, anti-*ouro2,* and anti-*Foxn1* TALEN constructs using the mMESSAGE mMACHINE SP6 kit (Ambion) and dissolved in Nuclease-Free Water (Ambion). Fertilized eggs were injected with 4 nl of 100-200 ng/μl each of TALEN mRNA and 25-50 ng/μl mCherry mRNA (Nakajima & Yaoita 2013). The embryos were raised at 22–24°C in 0.1 × MMR [MMR; 100 mM NaCl/2 mM KCl/2 mM $CaCl_2$/1 mM $MgCl_2$/5 mM HEPES (pH 7.4)] containing 0.1% BSA and 50 μg/ml gentamicin.

DNA purification

Ten three-day-old F0 embryos were homogenized in 180 µl of 50 mM NaOH and incubated for 10 min at 95°C. The homogenate was neutralized by 20 µl of 1 M Tris-Cl (pH 8.0) and centrifuged at 15,000 × g for 10 min at 4°C. The supernatant was mixed with phenol vigorously and centrifuged. The aqueous phase was transferred into a new tube, mixed with chloroform, and centrifuged. The aqueous phase was stored for PCR.

Genomic DNA was extracted from an amputated tail tip of an F1 tadpole using the SimplePrep reagent for DNA (TaKaRa) according to the manufacturer's instructions.

Mutation analysis

A DNA fragment containing the anti-*ouro1* TALEN target sites was amplified using the EmeraldAmp MAX PCR Master Mix (TaKaRa), genomic DNA from F0 embryos, and the primers (ouro1-F1 and ouro1-R1) with a three-step protocol [(95°C, 30 s; 55°C, 30 s; 72°C, 1 min) x 30]. The amplicon was subcloned into the pGEM-T Easy vector (Promega), and the nucleotide sequence was subsequently determined. A target DNA fragment of anti-ouro2 TALEN was amplified similarly using F0 genomic DNA and primers (ouro2-F1 and ouro2-R1) with a three-step protocol [(95°C, 30 s; 60°C, 30 s; 72°C, 1 min) x 30]. A target DNA fragment of anti-*Foxn1* TALEN was amplified using F0 genomic DNA and primers (Foxn1-F1 and Foxn1-R1) with the same protocol.

A target DNA fragment of anti-*ouro1* TALEN was amplified using F1 genomic DNA and primers (ouro1-F2 and ouro1-R2) with a three-step protocol [(95°C, 30 s; 60°C, 30 s; 72°C, 30 s) x 35]. The amplicon was recloned into the pGEM-T Easy

vector, and the nucleotide sequence was determined. When only one target sequence was observed in F1 DNA, PCR was performed using KOD DNA polymerase (TOYOBO) and primers (ouro1-F3 and ouro1-R3) with a three-step protocol {(95°C, 30 s; 60°C, 30 s; 72°C, 3 min 30 s) x 30}. A target DNA fragment of anti-*ouro2* TALEN was amplified using F1 DNA and primers (ouro2-F2 and ouro2-R2) with a three-step protocol [(95°C, 30 s; 60°C, 30 s; 72°C, 30 s) x 35]. A target DNA fragment of anti-*Foxn1* TALEN was amplified using F1 DNA and primers (Foxn1-F2 and Foxn1-R2) with the same protocol. The primer sequences used for mutation analysis are shown in Table 1.

Western blot analysis

Anti-Ouro1 and anti-Ouro2 serums were prepared by immunizing rabbits with the synthetic peptides QVKFDEDSGATKDL and SDSGFQKKESSTEL, respectively (GenScript) (Fig. 2 and 3). Tadpole skin was excised, homogenized and sonicated in SDS buffer (Okada *et al.* 2012), and 10 μg of protein was loaded and subjected to SDS-polyacrylamide gel electrophoresis. A blot was probed with the rabbit anti-Ouro1 or anti-Ouro2 antiserum diluted 1:1000. A phosphatase-labeled goat anti-rabbit IgG antibody (KPL) diluted 1:10,000 was used as a secondary antibody. Reactive bands were visualized by treatment with CDP-Star Chemiluminescence Reagent (PerkinElmer). A blot was stripped in 25 mM glycine (pH 2.5)-1% SDS for 30 s, followed by incubation with a rabbit anti-actin antibody (Sigma-Aldrich, A2066) diluted 1:1000 as a first antibody and a phosphatase-labeled goat anti-rabbit IgG

antibody as a secondary antibody.

Flow cytometry and immunofluorescence staining

Spleens were dissected from anesthetized frogs and broken up using a loose-fitting plastic homogenizer to prepare cell suspension. Immunofluorescence staining was performed as previously described (Nagata 1986). The spleen cells were reacted with undiluted hybridoma supernatant containing mouse monoclonal anti-*Xenopus* CD8 antibodies, AM22 and F17, from Xenopus research resource for immunobiology (https://www.urmc.rochester.edu/microbiology-immunology/xenopus-laevis.aspx), stained with 1:1000 dilution of Alexa Fluor 488 goat anti-mouse IgM (Life Technologies), and analyzed on a FACSCalibur flow cytometer (Becton Dickinson). Electronic gates were set by forward and side scatter to delineate lymphoid cells, 3000 to 6000 gated counts were accumulated, and the results are shown as histograms with the number of cells on the y-axis and logarithmic unit of fluorescence intensity on the x-axis.

Transplantation of skin graft

Ventral skin grafts (2 mm x 2 mm) were excised from both the Ivory Coast and the Nigerian H (Yasuda) strains of *X. tropicalis* frogs and transplanted to the dorsal side of the trunk of the wild-type and *Foxn1*-knockout frogs of the Ivory Coast strain. Frogs were maintained at 26 to 28°C. Photographs were taken every week.

Results

Developmental expression of *ouro1* and *ouro2* mRNA and proteins during *Xenopus tropicalis* (*X. tropicalis*) metamorphosis

We searched the *X. tropicalis* genome and cDNA database for *ouro1* and *ouro2* genes using the nucleotide and amino acid sequences of *X. laevis ouro* genes. Only one gene locus was found for *ouro1* and *ouro2* orthologs, respectively (Table 2). The sequence comparison between *X. laevis* and *X. tropicalis* revealed 88.3% and 92.2% identities for *ouro1* and *ouro2* genes, respectively, at the nucleotide level in the coding region and 90.2% and 90.7% identities for Ouro1 and Ouro2 proteins, respectively, at the amino acid level (Figs. 1 and 2). *ouro1* and *ouro2* mRNA are reportedly expressed in *X. laevis* tail skin from stage 50 to 62 (Mukaigasa *et al.* 2009). Our quantitative reverse transcription-polymerase chain reaction (qPCR) assay showed that both *ouro* mRNAs were observed in *X. tropicalis* tail skin until stage 60 but not at stage 63 (Fig. 4A,B). Skinned tail expressed less than 1/1500 of *ouro1* mRNA and 1/500 of *ouro2* mRNA compared to tail skin at stages 56, 58 and 60, which indicated the skin-specific expression of *ouro* mRNA in the tail.

Ouro proteins are known to be present in *X. laevis* tail skin at stages 54-64 but absent in trunk skin at stage 62. Western blot analysis revealed that the expression of Ouro proteins persisted until stage 64 in *X. tropicalis* tail skin, but Ouro1 protein was undetectable at stage 62 and Ouro2 was hardly observed in the back skin (Fig. 4C,D).

Taken together, these results indicated that the spatio-temporal expression patterns of *ouro* mRNA and proteins in *X. tropicalis* are similar to those in *X. laevis*.

Generation and analysis of *ouro1*-knockout tadpoles

Ouro protein contains a central rod domain flanked by N- and C-terminal glycine-serine rich domains. We designed anti-*ouro1* TALEN target sites in the first exon (Fig. 5A). The sites are located at the protein level in the N-terminal glycine-serine rich domain and upstream of the region that was to have T-cell proliferation activity in *X. laevis* (Mukaigasa *et al.* 2009) (Fig. 2A). The 100 kb region encompassing the *ouro2* genomic gene was searched for anti-*ouro1* TALEN target sites using the left and right recognition sequences 5'-CRRTRCTRRRRCTRRTCC-3' and 5'-RCTTRRCCCRRRRCCR-3' (where R is A or G), respectively, because a TALEN DNA binding repeat that recognizes the nucleotide G also binds to the nucleotide A. There were no sequences with eight or fewer mismatched nucleotides and 10 to 30 spacer nucleotides.

Pooled genomic DNA was extracted from ten F0 embryos three days after fertilization and TALEN mRNA injection to determine the *ouro1* mutation rate. All examined genes were modified (14/14) and contained in-frame (9/14) or out-of-frame mutations (5/14) (Fig. 6A). F0 embryos underwent normal metamorphosis and developed into sexually mature adult frogs. Four male and five female F0 frogs were mated to obtain offspring. The genotypes of 58 F1 frogs were determined and showed in-frame (75/116) and out-of-frame (32/116) mutations as well as a large deletion of 715 base pairs (bp) containing the initiation codon (9/116) (Table 3). The lower frequency of

out-of-frame mutations suggests that the out-of-frame mutations compromise the F1 survival rate, which may make it difficult to obtain *ouro1*-knockout frogs.

RNA and tissue lysates were prepared from the skin of stage 60 tadpole, with a deletion of 4 bp and an insertion of 15 bp in the *ouro1* coding region of one chromosome and a deletion of 715 bp on the other chromosome (Fig. 6B), and subjected to qPCR and Western blot analyses, respectively. The level of *ouro1* mRNA decreased to 1/26 and 1/50 in the *ouro1*-knockout tadpole tail compared with the stage 60 wild-type tadpole tails when qPCR was conducted using one pair of primers downstream and another pair upstream of the TALEN target sites, respectively (Fig. 5). The nonsense-mediated RNA decay (NMD) pathway may degrade mRNA transcribed from one *ouro1* gene with the out-of-frame mutation, and the low promoter activity may reduce transcription from the gene on the other chromosome, where the deleted region extends from more than 300 bp upstream of the initiation codon to approximately 400 bp downstream into the coding region. The expression level of *ouro2* mRNA was not affected in the knockout tail skin.

The protein analysis revealed that Ouro1 protein was absent in the tail and back skin of the stage 60 *ouro1*-knockout tadpole, and Ouro2 protein was also scarcely detected in the tail skin (Fig. 5C,D). The hagfish counterparts of Ouro proteins, thread keratin and , form a stable complex *in vitro* (Schaffeld & Schultess 2006). It is possible that the Ouro2 protein was destroyed by the protein quality control mechanism because it may fail to fold correctly due to the absence of its normal partner protein Ouro1. The results showed that both the out-of-frame mutation and a large deletion of

the *ouro1* gene prevented the translation of intact Ouro1 protein and reduced the expression level of Ouro2 protein.

Prominent tail regression is observed between stages 62 and 65 in wild-type tadpoles, when the tail is reduced in three days from 30 mm long to 1 mm long (Fig. 12A). Tadpoles are staged from stage 63 to 65 based on the ratio of tail length to body length. We examined five tadpoles with biallelically different out-of-frame mutations (out/out) or an out-of-frame mutation and a large deletion (out/Ldel) (Fig. 6B). There was no significant difference in the time required for the tail shortening from stage 62 to 65 between wild-type and *ouro1*-knockout tadpoles (Fig. 12B), and only no-tailed frogs were obtained (Fig. 13), indicating that neither the Ouro1 nor the Ouro2 protein is necessary for tadpole tail regression.

Generation and analysis of *ouro2*-knockout tadpoles

An anti-*ouro2* TALEN was designed to target the first exon (Fig. 7A). The target sites are located at the juncture between the N-terminal glycine-serine rich and the central rod domains and in the region that is expected from the analysis of *X. laevis* (Mukaigasa *et al.* 2009) to have T cell proliferation activity (Fig. 2B). No sequences similar to the anti-*ouro2* TALEN target sites were found with eight or fewer mismatched nucleotides and 10 to 30 spacer nucleotides within 340 kb of the genomic DNA region containing the *ouro1* gene.

Wild-type *ouro2* sequences (2/26), in-frame mutations (13/26) and out-of-frame mutations (11/26) were observed by analyzing pooled genomic DNA

derived from ten three-day-old F0 tadpoles that had been injected with anti-*ouro2* TALEN mRNA (Fig. 8A). The mating of six male and two female F0 frogs generated 47 offspring that harbored wild-type *ouro2* sequences (32/94), in-frame mutations (9/94), and out-of-frame mutations (53/94) (Table 3). RNA and tissue lysates were prepared from the skin of the stage 60 tadpole, with a deletion of 2 bp in the *ouro2* gene on one chromosome and a deletion of 8 bp on the other chromosome (Fig. 8B), and subjected to RNA and protein analyses, respectively. qPCR analysis showed the reduction of *ouro2* mRNA to 1/32 and 1/64, using a pair of primers downstream and another pair upstream of the target sites, respectively, in the tail skin of the *ouro2*-knockout tadpole compared with wild-type tadpoles (Fig. 7B). A low level of *ouro2* mRNA may be ascribed to the NMD pathway. In Western blot analysis, Ouro2 protein was undetectable in the tail and back skin of the *ouro2*-knockout tadpole and Ouro1 protein was hardly observed (Fig. 7C,D). The latter can be explained by the protein quality control mechanism described above and by the reduced level of *ouro1* mRNA due to unknown reasons. Our results demonstrated that Ouro1 protein expression was very low, and intact Ouro2 protein was not detected in the *ouro2*-knockout tadpole tail and back skin.

All the examined *ouro2*-knockout tadpoles exhibited shortened tails during the metamorphosis climax without any significant delay, similar to the wild-type and wt/out mutant (Fig. 12B), and did not retain any tail after the completion of metamorphosis (Fig. 13), demonstrating that neither the Ouro1 nor the Ouro2 protein is required for tadpole tail regression.

Generation and analysis of *Foxn1*-knockout tadpoles

Anti-*Foxn1* TALEN was constructed to examine whether the immunological rejection by T cells and more particularly CD8 cytotoxic T cells plays a pivotal role in tadpole tail regression. The mutation of *Foxn1* should lead to a phenotype similar to that of a nude mouse, which shows a congenital loss of the thymus and mature T cells, including helper and cytotoxic T cells and, therefore, the defect of immunological rejection by $CD8^+$ cytotoxic T cells (Nehls *et al.* 1994). Anti-*Foxn1* TALEN target sites were designed in the seventh exon. At the protein level, the sites are located in the DNA-binding domain and upstream of the transcriptional activation domain (Fig. 9A). The *Foxn1* gene was analyzed using pooled genomic DNA derived from ten three-day-old F0 tadpoles. All genes were modified and harbored in-frame (2/12) or out-of-frame (10/12) mutations (Fig. 10A). The thymus is easy to observe in the head region of living tadpoles after stage 52 (Fig. 9B). We chose three male and three female F0 frogs that had no thymus and mated them. Only athymic F1 tadpoles were selected and subjected to genotype analysis. Fourteen of 27 tadpoles contained biallelically different out-of-frame mutations (Fig. 10B). As the tadpoles with wt/out, in/in, and in/out mutations had no thymus, some out-of-frame and in-frame of mutations might interfere with gene function as a dominant-negative inhibitor (Table 3).

Fluorescein-activated cell sorter analysis using monoclonal antibodies against *Xenopus* CD8, AM22 and F17 revealed a loss of $CD8^+$ cells in the spleen of a frog (#13) with biallelically different out-of-frame mutations (Fig. 10B), whereas there were

$CD8^-$ and $CD8^+$ peaks in the splenic cells of wild-type frogs (Fig. 9C). *Foxn1*-knockout tadpoles underwent metamorphosis normally and proceeded from stage 62 to 65 in approximately three days without any delay compared to wild-type tadpoles (Fig. 12B) and did not have a tail after the completion of metamorphosis (Fig. 13).

To confirm the impaired immunological rejection in *Foxn1*-knockout frogs, we examined the ability to reject a transplanted skin graft from a different strain. The Ivory Coast frog strain rejects transplanted skin grafts from the Nigerian H (Yasuda) strain (Kashiwagi *et al.* 2010). White ventral skin grafts of Ivory Coast and Nigerian H strains were transplanted to the backs of wild-type and *Foxn1*-knockout Ivory Coast frogs. Ivory Coast recipients acutely rejected skin grafts from Nigerian H donors within 13.1 days ± 1 at 26°C (n = 5), indicating a major histocompatibility (MHC)-disparate rejection, whereas slower chronic rejection (68.6 days ± 7.7; n = 5) occurred when skin grafts from Ivory Coast donors were transplanted onto Ivory Coast recipients, which implies minor histocompatibility-disparate rejection. In sharp contrast, neither MHC-mismatched Nigerian H nor minor histocompatibility-mismatched Ivory Coast skin transplants were rejected by *Foxn1*-knockout #2 and #3, which survived for as long as 105 days at 26°C (Fig. 9D and Fig. 11). *Foxn1*-knockout #2 and #3 harbored the biallelically different out-of-frame mutations (Fig.10B), and developed from stage 62 to 65 in three days. Three other knockout recipients were fully tolerant to skin transplants from Nigerian H donors but showed ambiguous reaction to skin transplants from Ivory Coast donors characterized by inflammation with heavy vascularization in the grafted tissue at early time points and different degree of melanophore infiltration. Such

allogeneic responses may be mediated by NK cells or other innate immune cell effectors as reported for T cell deficient mouse (Kroemer *et al.* 2008; Zecher *et al.* 2009).

Discussion

Ouro proteins are not necessary for tail regression in *X. tropicalis*

Our *ouro1*- and *ouro2*-knockout tadpoles showed no delay in tail regression during the climax and did not retain a tail after the completion of metamorphosis, which clearly demonstrated that neither the *ouro1* nor *ouro2* gene is necessary for tail regression.

The *ouro2* gene should not be modified in *ouro1*-knockout tadpoles, as we could not find any sequence with eight or fewer mismatched nucleotides in the 100 kb region containing the *ouro2* gene, compared with the target sites (18 bp and 16 bp) of the anti-*ouro1* TALEN. Therefore, anti-Ouro2 antibody can recognize all expressed Ouro2 protein, and the protein analysis showed a very low expression level of Ouro2 in the *ouro1*-knockout tadpole tail. However, we cannot exclude the possibility of the expression of a truncated N-terminal Ouro1 protein because our anti-Ouro1 antibody was prepared by immunizing a synthetic peptide located downstream of the anti-*ouro1* TALEN target sites. When an out-of-frame mutation was introduced by TALEN, it may have resulted in the premature termination and synthesis of the truncated N-terminal protein that contains only the glycine-serine rich domain but not the central rod domain with adult T cell proliferation activity (Mukaigasa *et al.* 2009). Our finding that an upstream part of *ouro1* mRNA also decreased to 1/50 corroborated that the truncated Ouro1 protein was expressed at a very low level, if it was produced at all. The same argument applies to the *ouro2*-knockout frogs.

Our conclusion is inconsistent with a previous report that the knockdown of

ouro expression by heat-inducible antisense *ouro* RNA delayed tail shortening and generated tailed frogs using *X. laevis* transgenic tadpoles (Mukaigasa *et al.* 2009). The authors of that report presented the results of *ouro* mRNA and protein analyses using a heat-shocked tail, but the RT-PCR result was not quantitative, and many Ouro2 signals were still observed in the immunostaining of the tail tip of the *ouro2*-knockdown tadpole. In spite of the low efficiency of the *ouro2* knockdown, tail shortening was delayed significantly after the heat shock of the stage 58/59 transgenic tadpoles. In our study, the targeted *ouro* genes were modified or deleted to extinguish the gene function, the expression levels of the mRNA were reduced to 1/26-1/64, and the translated proteins of targeted and non-targeted *ouro* genes were expressed at undetectable and very low levels, respectively. In these conditions, a delay of tail regression and retained tails were not observed. It is possible that the active apoptotic pathway in the regressing tail was hindered by the harmful effect of heat shock in the previous authors' experiments. Our results clearly demonstrated that Ouro proteins are not essential to tail regression. However, we cannot exclude the possibility that this discrepancy is ascribed to the difference between *X. tropicalis* and *X. laevis*, that unknown molecules other than Ouro proteins act as larval antigens for the immunological rejection in our knockout tadpoles, or that antisense *ouro* RNA not only inhibits *ouro* gene expression but also incidentally influences the expression of genes that are important to tail regression.

The mechanism of tadpole tail regression

Tail muscle cell death is detected and the tip of the tail begins to atrophy at stage 58

(Nakajima & Yaoita 2003; Nieuwkoop & Faber 1956; Nishikawa & Hayashi 1995), which indicates that tail degeneration starts at the beginning of the metamorphosis climax, that is, before the immunological rejection system is established. Only cell-autonomous death (suicide) by TH signaling could be responsible for the early change.

Tail fins are reduced considerably and the notochord begins to degenerate posteriorly at stage 61 (Nieuwkoop & Faber 1956). ECM-degrading enzymes are expressed abruptly in the tail starting at stage 62 (Fujimoto *et al.* 2007). Tail shortening also starts at stage 62. It is possible that all the mechanisms based on the suicide, murder, and immunological rejection models collaborate to eliminate a tail during the latter half of the metamorphosis climax. However, our results argue against the immunological rejection model.

In the immunological rejection model, it is not known which immune cells kill tail cells. $CD8^+$ cells were not required in normal tail regression during the metamorphosis climax in the congenital athymic *Foxn1*-knockout tadpoles with undetectable levels of $CD8^+$ cells in the spleen. This finding excludes the possibility that cytotoxic immune cells such as conventional MHC class Ia-restricted $CD8^+$ cytotoxic T cells (CTLs), classical class Ia-unrestricted CTLs, and natural killer T cells play a pivotal role in tail rejection because these cells are all CD8-positive (Edholm *et al.* 2014). Natural killer cells fail to kill class Ia-deficient tumor cells before and after metamorphosis, suggesting that they have no cytotoxic activity during metamorphosis (Horton *et al.* 2003). Recently, nonclassical MHC class I-dependent invariant T cells (iT

cells) have been reported to show *in vivo* cytotoxicity in tadpoles against tumor cells that are deficient in both class Ia and class Ib XNC10 (Edholm *et al.* 2013). iT cells are classified into type I and type II. Type I iT cells are CD8/CD4 double negative, and type II cells have a lower level of CD8 expression compared with conventional T cells. Type I iT cells may be good candidates for eliminating the tail, although they develop in the thymus.

The congenital loss of thymus by the modification of *Foxn1* gene should result in the absence of all T cells containing not only $CD8^+$ cytotoxic T cells, but also $CD4^+$ helper T cells and iT cells. This should also lead to the compromised cytokine-mediated cell-cell interaction and the failure of adaptive immunity in knockout animals. The normal tail regression in *Foxn1*-knockout tadpoles strongly suggest that adaptive immunity is not involved in the tail elimination.

While the impairment of skin allograft rejection provides a strong evidence of the T cell deficiency of *Foxn1*-knockout frogs, the occurrence of unconventional inflammation-associated rejection patterns by some *Foxn1*-knockout recipients for skin of one of the two donor genotypes (Ivory Coast) suggests an alloreaction by innate immune cell effectors such as NK cells and/or monocytes. As such, we cannot exclude the possibility that some of these innate immune effector cells are involved in the elimination of the tail during metamorphic climax. However, wild-type *X. tropicalis* tadpoles proceed from stage 60 to 65 in nine days in our laboratory without obvious inflammation, heavy vascularization, and bleeding in the tail. Moreover, our study clearly demonstrates that larval-skin-specific Ouro proteins are not essential to tail

regression. Thus, we believe that it is important to reexamine the immunological rejection model that is based on the observation that tadpole skin grafts are rejected by isogenic frogs.

Acknowledgements

I would like to express my sincere gratitude to my supervisor, Professor Yoshio Yaoita (Institute for Amphibian Biology, Hiroshima University) for valuable discussion, guidance and thought encouragements. I also would like to express thank to Dr. Keisuke Nakajima and Ichiro Tazawa (Institute for Amphibian Biology, Hiroshima University) for technical advice and thought encouragements.

References

Berry, D.L., Schwartzman, R.A. & Brown, D.D. (1998) The expression pattern of thyroid hormone response genes in the tadpole tail identifies multiple resorption programs. *Dev. Biol*. **203**, 12-23.

Brown, D.D., Wang, Z., Furlow, J.D., *et al*. (1996) The thyroid hormone-induced tail resorption program during *Xenopus laevis* metamorphosis. *Proc. Natl. Acad. Sci. U.S.A.* **93**, 1924-1929.

Cermak, T., Doyle, E.L., Christian, M., *et al*. (2011) Efficient design and assembly of custom TALEN and other TAL effector-based constructs for DNA targeting. *Nucleic Acids Res*. **39**, e82.

Das, B., Schreiber, A.M., Huang, H. & Brown, D.D. (2002) Multiple thyroid hormone-induced muscle growth and death programs during metamorphosis in *Xenopus laevis*. *Proc. Natl. Acad. Sci. U.S.A.* **99**, 12230-12235.

Edholm, E.S., Albertorio Saez, L.M., Gill, A.L., *et al*. (2013) Nonclassical MHC class I-dependent invariant T cells are evolutionarily conserved and prominent from early development in amphibians. *Proc. Natl. Acad. Sci. U.S.A.* **110**, 14342-14347.

Edholm, E.S., Grayfer, L. & Robert, J. (2014) Evolution of nonclassical MHC-dependent invariant T cells. *Cell. Mol. Life Sci*. **71**, 4763-4780.

Elinson, R.P., Remo, B. & Brown, D.D. (1999) Novel structural elements identified during tail resorption in *Xenopus laevis* metamorphosis:Lessons from tailed frogs. *Dev.*

Biol. **215**, 243-252.

Fujimoto, K., Nakajima, K. & Yaoita, Y. (2006) One of the duplicated matrix metalloproteinase-9 genes is expressed in regressing tail during anuran metamorphosis. *Dev. Growth Differ.* **48**, 223-241.

Fujimoto, K., Nakajima, K. & Yaoita, Y. (2007) Expression of matrix metalloproteinase genes in regressing or remodeling organs during amphibian metamorphosis. *Dev. Growth Differ.* **49**, 131-143.

Hertwig, O. (1898) Uber den Einfluss der Temperature auf die Entwicklung von *Rana fusca* und *Rana esculenta*. *Arch. Mikorosk. Anat*. **51**, 319-381.

Horton, T.L., Stewart, R., Cohen, N.*, et al*. (2003) Ontogeny of *Xenopus* NK cells in the absence of MHC class I antigens. *Dev. Comp. Immunol*. **27**, 715-726.

Huang, H., Marsh-Armstrong, N. & Brown, D.D. (1999) Metamorphosis is inhibited in transgenic *Xenopus laevis* tadpoles that overexpress type III deiodinase. *Proc. Natl. Acad. Sci. U.S.A*. **96**, 962-967.

Izutsu, Y. & Yoshizato, K. (1993) Metamorphosis-dependent recognition of larval skin as non-self by inbred adult frogs (*Xenopus laevis*). *Journal of experimental zoology* **266**, 163-167.

Kashiwagi, K., Kashiwagi, A., Kurabayashi, A.*, et al*. (2010) *Xenopus tropicalis*: an ideal experimental animal in amphibia. *Exp. Anim*. **59**, 395-405.

Kroemer, A., Xiao, X., Degauque, N.*, et al*. (2008) The innate NK cells, allograft rejection, and a key role for IL-15. *J. Immunol*. **180**, 7818-7826.

Lei, Y., Guo, X., Liu, Y.*, et al*. (2012) Efficient targeted gene disruption in *Xenopus*

embryos using engineered transcription activator-like effector nucleases (TALENs). *Proc. Natl. Acad. Sci. U.S.A.* **109**, 17484-17489.

Mukaigasa, K., Hanasaki, A., Maeno, M., *et al*. (2009) The keratin-related Ouroboros proteins function as immune antigens mediating tail regression in *Xenopus* metamorphosis. *Proc. Natl. Acad. Sci. U.S.A.* **106**, 18309-18314.

Nagata, S. (1986) Development of T lymphocytes in *Xenopus laevis*: appearance of the antigen recognized by an anti-thymocyte mouse monoclonal antibody. *Dev. Biol.* **114**, 389-394.

Nakajima, K., Fujimoto, K. & Yaoita, Y. (2005) Programmed cell death during amphibian metamorphosis. *Semin. Cell Dev. Biol.* **16**, 271-280.

Nakajima, K., Nakai, Y., Okada, M. & Yaoita, Y. (2013) Targeted Gene Disruption in the *Xenopus tropicalis* Genome using Designed TALE Nucleases. *Zool. Sci.* **30**, 455-460.

Nakajima, K. & Yaoita, Y. (2003) Dual mechanisms governing muscle cell death in tadpole tail during amphibian metamorphosis. *Dev. Dyn.* **227**, 246-255.

Nakajima, K. & Yaoita, Y. (2013) Comparison of TALEN scaffolds in *Xenopus tropicalis*. *Bio. Open* **2**, 1364-1370.

Nehls, M., Pfeifer, D., Schorpp, M., Hedrich, H. & Boehm, T. (1994) New member of the winged-helix protein family disrupted in mouse and rat nude mutations. *Nature* **372**, 103-107.

Nieuwkoop, P.D. & Faber, J. (1956) Normal table of *Xenopus laevis*, Amsterdam, North-Holland Publishing Company.

Nishikawa, A. & Hayashi, H. (1995) Spatial, temporal and hormonal regulation of programmed muscle cell death during metamorphosis of the frog *Xenopus laevis*. *Differentiation* **59**, 207-214.

Okada, M., Nakajima, K. & Yaoita, Y. (2012) Translational regulation by the 5'-UTR of thyroid hormone receptor α mRNA. *J. Biochem.* **151**, 519-531.

Schaffeld, M. & Schultess, J. (2006) Genes coding for intermediate filament proteins closely related to the hagfish "thread keratins (TK)" alpha and gamma also exist in lamprey, teleosts and amphibians. *Exp. Cell Res.* **312**, 1447-1462.

Watanabe, M., Ohshima, M., Morohashi, M., Maeno, M. & Izutsu, Y. (2003) Ontogenic emergence and localization of larval skin antigen molecule recognized by adult T cells of *Xenopus laevis*: Regulation by thyroid hormone during metamorphosis. *Dev. Growth Differ.* **45**, 77-84.

Weber, R. (1962) Induced metamorphosis in isolated tails of *Xenopus* larvae. *Experientia* **18**, 84-85.

Yaoita, Y. & Nakajima, K. (1997) Induction of apoptosis and CPP32 expression by thyroid hormone in a myoblastic cell line derived from tadpole tail. *J. Biol. Chem.* **272**, 5122-5127.

Zecher, D., van Rooijen, N., Rothstein, D.M., Shlomchik, W.D. & Lakkis, F.G. (2009) An innate response to allogeneic nonself mediated by monocytes. *J. Immunol.* **183**, 7810-7816.

Figures and tables

(A)

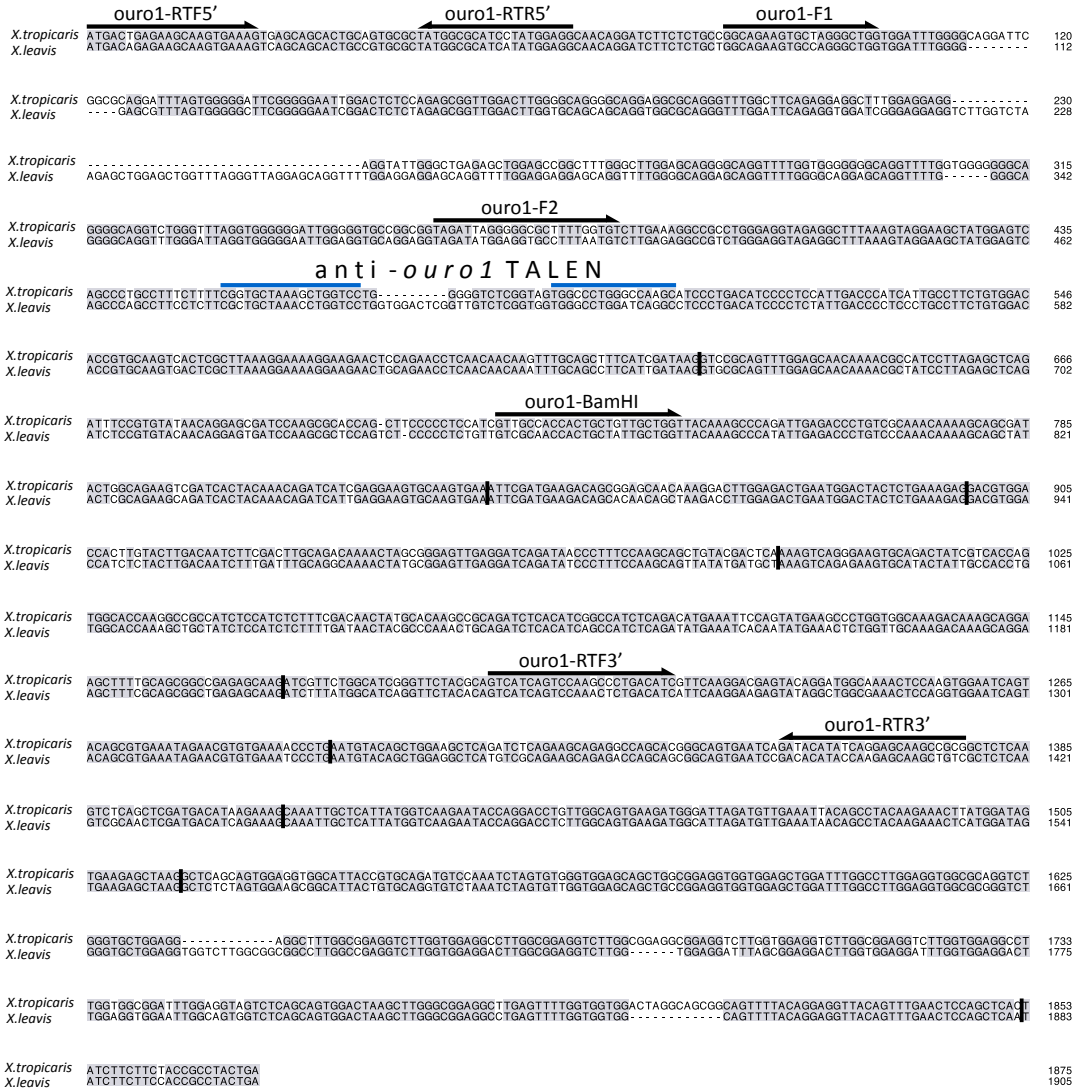
ouro1-RTF5'
ouro1-RTR5'
ouro1-F1
ouro1-F2
anti-ouro1 TALEN
ouro1-BamHI
ouro1-RTF3'
ouro1-RTR3'
X.tropicaris
X.leavis

(B)

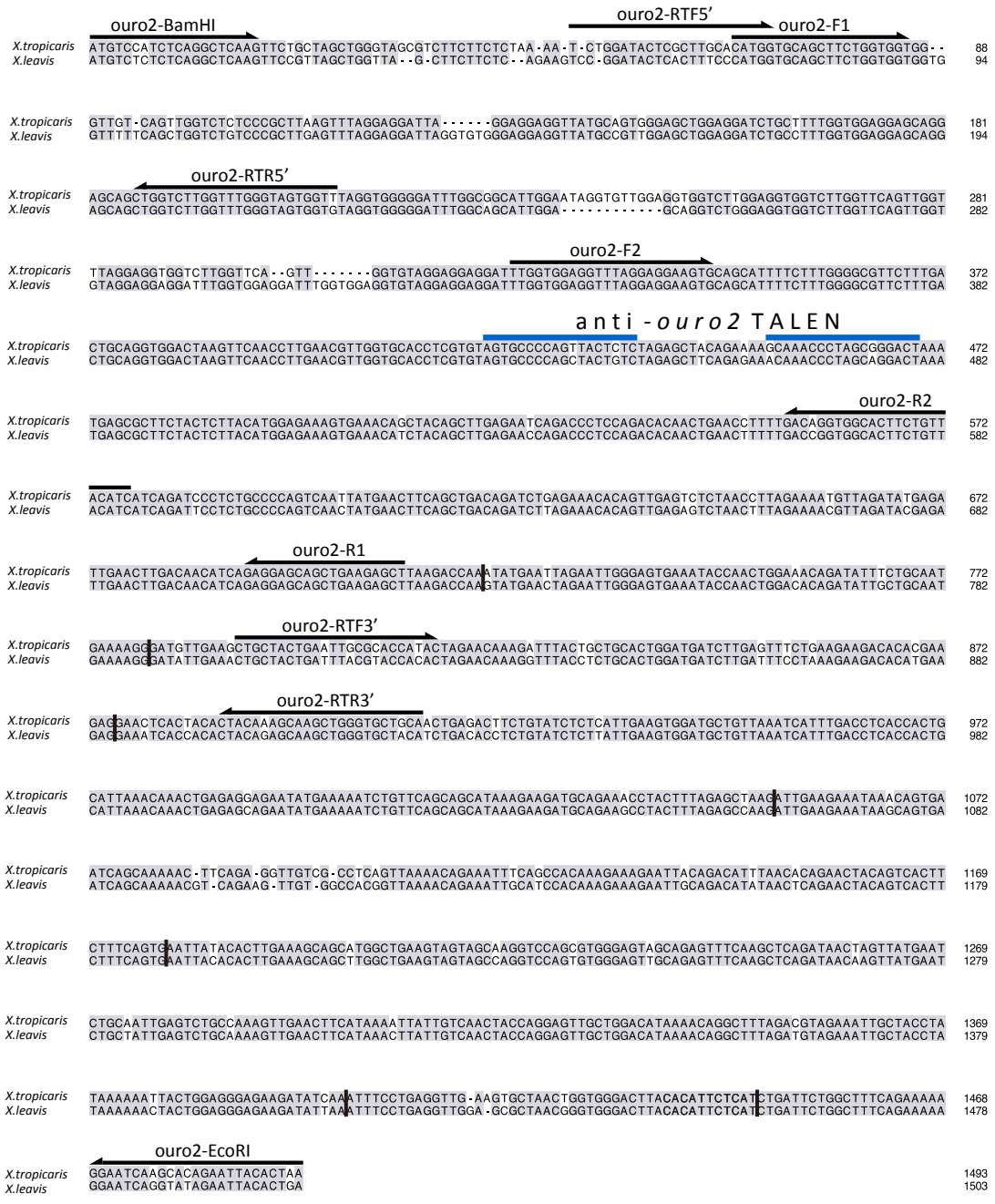

Fig. 1. Comparison between *X. tropicalis* and *X. laevis* nucleotide sequences of *ouro* coding region.

Conserved nucleotide sequences of *ouro1* (A) and *ouro2* (B) between *X. tropicalis* and *X. laevis* are shaded. Blue lines on *X. tropicalis* sequence denote the target sites of anti-*ouro* TALEN. Vertical lines indicate the intron insertion sites. Hyphens indicate nucleotide gaps. The positions of primers used in this experiment are shown.

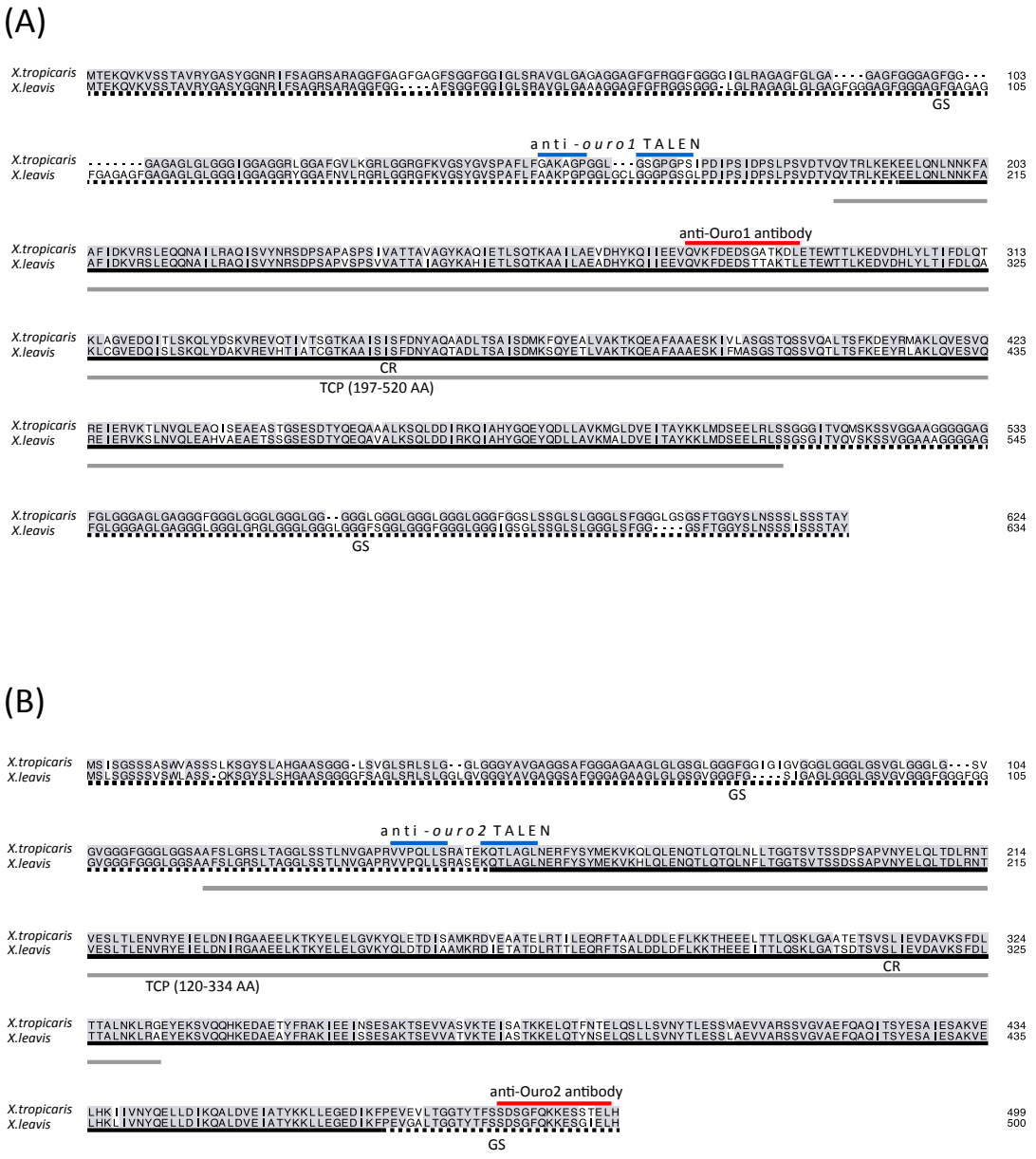

Fig. 2. Comparison between *X. tropicalis* and *X. laevis* Ouro protein sequences. Conserved amino acid sequences of Ouro1 (A) and Ouro2 (B) between *X. tropicalis* and *X. laevis* are shaded. Blue and red lines on *X. tropicalis* Ouro sequence denote the target sites of anti-*ouro* TALEN and the peptide sequence to prepare anti-Ouro antibody, respectively. Dotted black, solid black and solid gray lines under *X. laevis* Ouro sequence indicate the glycine-serine rich domains (GS), central rod domain (CR), and polypeptide with the T-cell proliferation activity (TCP), respectively.

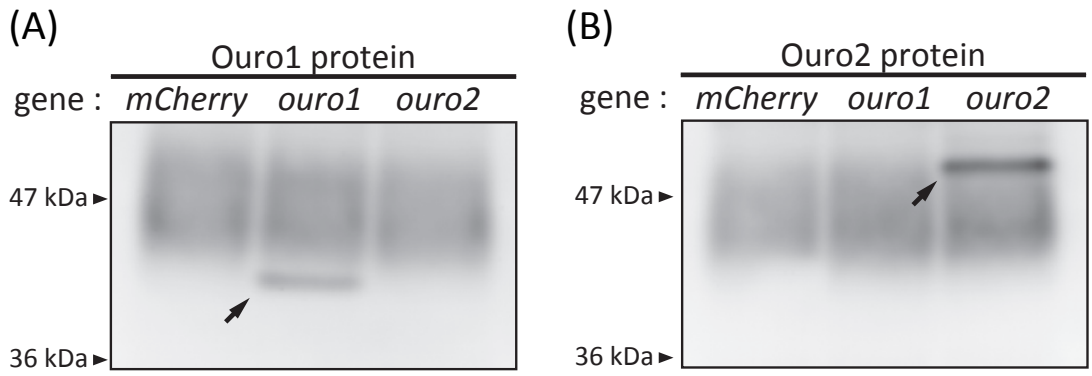

Fig. 3. Specificity of anti-Ouro antiserums.

As we failed to clone the full-length cDNA of *X. tropicalis ouro1* gene, the truncated *ouro1* gene was obtained instead. The truncated *ouro1* and full-length *ouro2* genes of *X. tropicalis* were amplified using the primers ouro1-BamHI and ouro1-EcoRI, and ouro2-BamHI and ouro2-EcoRI, respectively, digested with BamHI and EcoRI, and inserted into pCMV-Script. The DNA fragment containing T3 promoter, *mCherry* coding region, and poly A was prepared by PCR using the primers T3-pCMV and mCherry-pT, and pmCherry-N1 (Promega) as a template. The fragment containing T3 promoter, coding region of truncated *ouro1* or full-length *ouro2*, and poly A were amplified with the primers T3-pCMV and pCMV3'pT for *in vitro* transcription and translation using TNT T3 Coupled Reticulocyte Lysate System (Promega). 2.5 μl of reaction mixture including mCherry, truncated Ouro1 (41 kDa), or Ouro2 (50 kDa) protein was loaded in each lane. (*A* and *B*) Western blots showing the specificity of anti-Ouro1 (A) and anti-Ouro2 (B) antiserums. The bands of truncated Ouro1 and Ouro2 proteins were indicated by arrows.

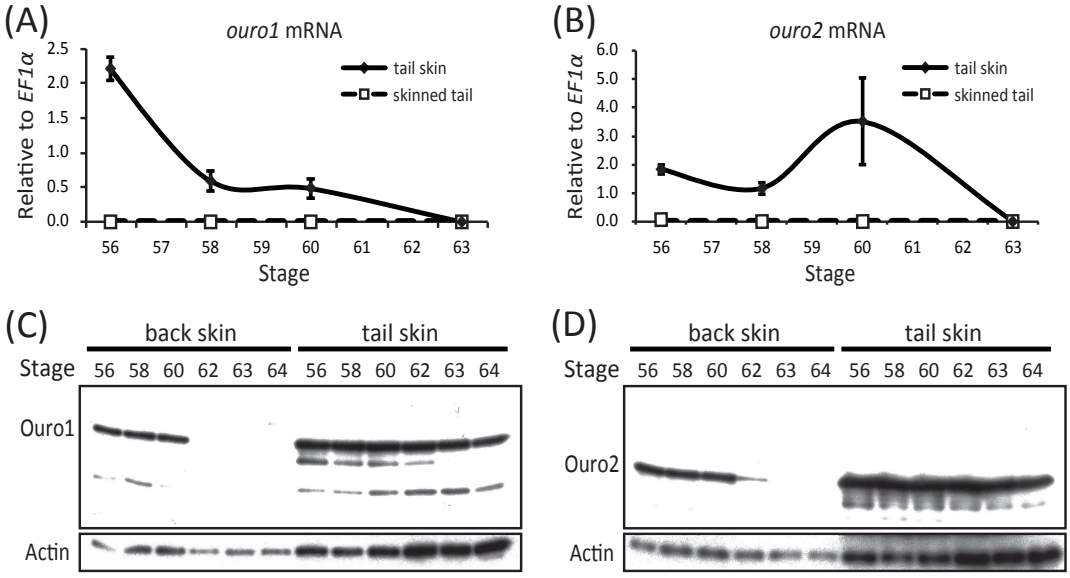

Fig. 4. Developmental expression of *ouro1* and *ouro2* mRNA and proteins during *X. tropicalis* metamorphosis.

(A, B) The expression levels of *ouro1* mRNA (A) and *ouro2* mRNA (B) in tail skin (solid line) and skinned tail (dotted line) from stage 56 to 63. Data are expressed as the means ± s.e.m. (N = 3 to 6). (C, D) Western blots showing the expression levels of Ouro1 protein (C) and Ouro2 protein (D) in back and tail skin from stage 56 to 6

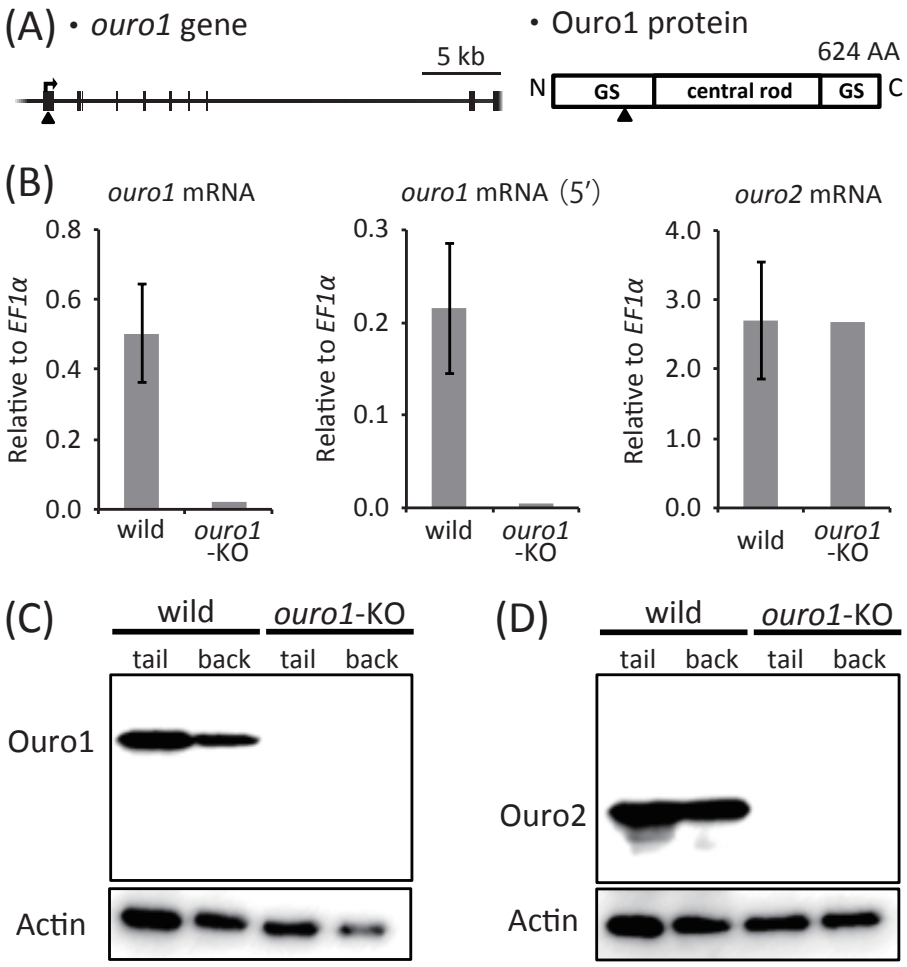

Fig. 5. Characterization of the *ouro1*-knockout tadpole.

(A) The target sites (arrowheads) of anti-*ouro1* TALEN in *ouro1* genomic gene and Ouro1 protein. The black boxes and the arrow indicate exons and the transcriptional direction, respectively. (B) Expression levels of *ouro1* and *ouro2* mRNA in the tail skin of stage 60 wild-type and *ouro1*-knockout tadpoles. Levels of *ouro1* mRNA were determined using a pair of primers downstream and another pair of primers (5') upstream of the TALEN target sites. Data from wild-type tadpoles are expressed as the means ± s.e.m. (N = 6). (C, D) Expression levels of Ouro1 (C) and Ouro2 (D) proteins in the tail and back skin of stage 60 wild-type and *ouro1*-knockout tadpoles.

(A)

TTTCGGTGCTAAAGCTGGTCCTGGGGGTCTCGGTAGTGGCCCTGGGCCAAGCATC	wild-type *ouro1*	
TTTCGGTGCTAAAG----------GTGGCCCTGGGCCAAGCATC	Δ21	x2
TTTCGGTGCTAAAGCTGGTCCTGG------CGGTAGTGGCCCTGGGCCAAGCATC	Δ6	x2
TTTCGGT----------AGTGGCCCTGGGCCAAGCATC	Δ27	
TTTCGGTGCTAAAGCTGGTCCTGGG----------CCAAGCATC	Δ21	
TTTCGGTGCTAAAGCTGGTCCT----------AGTGGCCCTGGGCCAAGCATC	Δ12	
TTTCGGTGCTAAAGCTGGTCC----------GGTAGTGGCCCTGGGCCAAGCATC	Δ10	
TTTCGGTGCTAAAGCTGGTCCTGG---------TAGTGGCCCTGGGCCAAGCATC	Δ9	
TTTCGGTGCTAAAGCTGGTCCTGGG--------TAGTGGCCCTGGGCCAAGCATC	Δ8	
TTTCGGTGCTAAAGCTGGTCCTGGGGG-------AGTGGCCCTGGGCCAAGCATC	Δ7	
TTTCGGTGCTAAAGCTGGTCCTGGGG-------TAGTGGCCCTGGGCCAAGCATC	Δ7	
ATTCGGTGCTAAAGCTGGTCCTGGGGG---CGGTAGTGGcCCTGGGCCAAGCATC	Δ3	
TTTCGGTGCTAAAGCTGGTCCTGGGG--CTCGGTAGTGGCCCTGGGCCAAGCATC	Δ2	

(B)

	TTTCGGTGCTAAAGCTGGTCCTGGGGGTCTCGGTAGTGGCCCTGGGCCAAGCATC	genotype		analysis
#1	TTTCGGTGCTAAAGCTGGTCCTGGG--------TAGTGGCCCTGGGCCAAGCATC TTTCGGTGCTAAAGCTGGTCCTGGGGG-----GTAGTGGCCCTGGGCCAAGCATC	Δ8 Δ5	out/out	tail regression
#2	TTTCGGTGCTAAAGCTGGTCCTGGG--------TAGTGGCCCTGGGCCAAGCATC TTTCGGTGCTAAAGCTGGTCCTGGGGG-----GTAGTGGCCCTGGGCCAAGCATC	Δ8 Δ5	out/out	tail regression
#3	TTTCGGTGCTAAAGCTGGTCCTGGG--------TAGTGGCCCTGGGCCAAGCATC TTTCGGTGCTAAAGCT----------AAAGTGGCCCTGGGCCAAGCATC	Δ8 Δ18+2	out/out	
#4	TTTCGGTGCTAAAGCTGGTCCTGGG--------TAGTGGCCCTGGGCCAAGCATC TTTCGGTGCTAAAGCTGGTCCTGGGG----TGGTAGTGGCCCTGGGCCAAGCATC	Δ8 Δ5+1	out/out	tail regression
#5	TTTCGGTGCTAAAGCTGGTCCTGGGGTAGTGGCCAGTGGTCCGGTAGTGGCCCTGGGCCAAGCATC Long deletion of 715 bp containing the initiation codon.	Δ4+15 Δ715	out/Ldel	qPCR Western blot
#6	TTTCGGTGCTAAAGCTGGTCCTGGGG-------TAGTGGCCCTGGGCCAAGCATC Long deletion of 715 bp containing the initiation codon.	Δ7 Δ715	out/Ldel	tail regression
#7	TTTCGGTGCTAAAGCTGGTCCTGGGG-------TAGTGGCCCTGGGCCAAGCATC TTTCGGTGCTAAAGCTGGTCCTGGG--------TAGTGGCCCTGGGCCAAGCATC	Δ7 Δ8	out/out	tail regression

Fig. 6. Nucleotide sequences of the *ouro1* gene derived from F0 and *ouro1*-knockout F1.

(A) Mutation analysis of F0 injected with anti-*ouro1* TALEN mRNA. The target DNA fragment was amplified using pooled genomic DNA purified from ten three-day-old F0 embryos and recloned for sequence determination. The mutation types are shown on the right. (B) Mutation analysis of *ouro1*-knockout F1. The target DNA fragment was amplified using genomic DNA purified from the amputated tail tip of F1 obtained by mating F0 frogs and recloned for sequence determination. The identity numbers of F1 tadpoles are represented in the left. Red characters indicate the inserted nucleotides (+). out, out-of-frame mutation; Ldel, a large deletion of 715 bp containing the initiation codon. Genotypes and analyses using F1 tadpoles are shown in the right. The wild-type target DNA sequence is indicated at the top. A pair of blue bars denotes the TALEN-binding sites. Hyphens indicate the gaps resulting from a deletion (Δ).

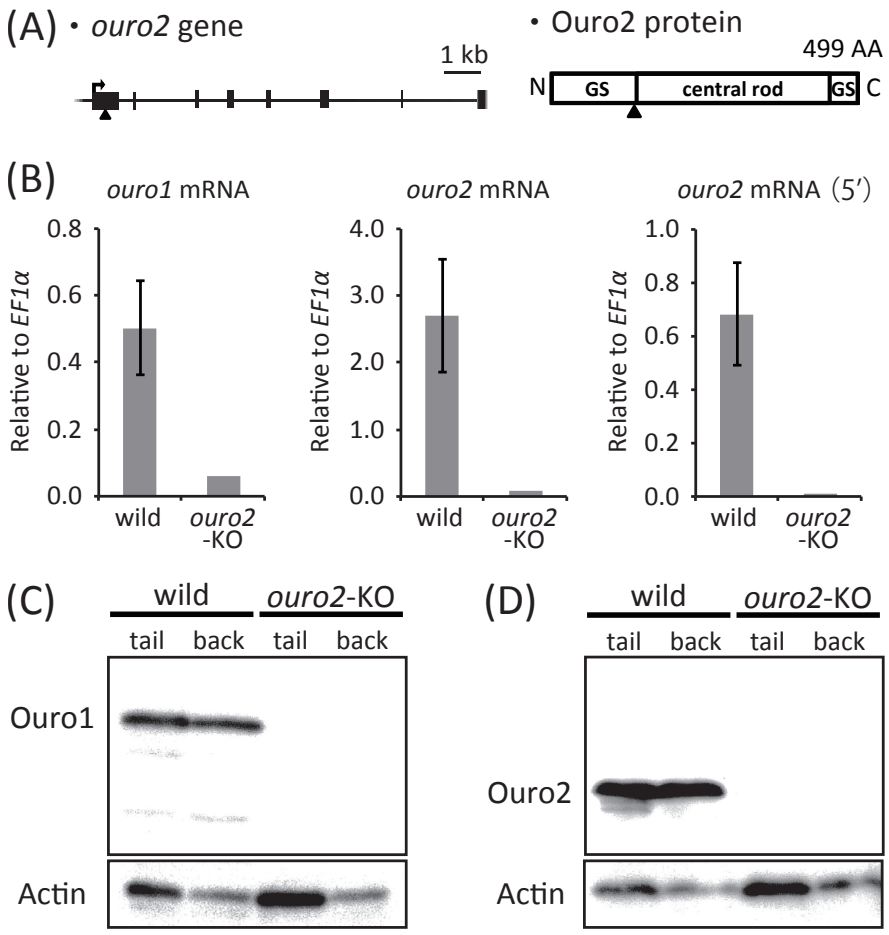

Fig. 7. Characterization of the *ouro2*-knockout tadpole.

(A) The target sites of anti-*ouro2* TALEN in *ouro2* genomic gene and Ouro2 protein. The alignment is labeled as described in the legend to Fig. 5. (B) Expression levels of *ouro1* and *ouro2* mRNA in tail skin of stage 60 wild-type and *ouro2*-knockout tadpoles. Levels of *ouro2* mRNA were determined using a pair of primers downstream and another pair of primers (5') upstream of the TALEN target sites. Data from wild-type tadpoles are expressed as the means ± s.e.m. (N = 6). (C, D) Expression levels of Ouro1 (C) and Ouro2 (D) proteins in the tail and back skin of stage 60 wild-type and *ouro2*-knockout tadpoles.

(A)

TGTAGTGCCCCAGTTACTCTCTAGAGCTACAGAAAAGCAAACCCTAGCGGGACTAAA	wild-type *ouro2*	
TGTAGTGCCCCAGTTACTCTCTAGAGCTACAGAAAAGCAAACCCTAGCGGGACTAAA	wild type	x2
TGTAGTGCCCCAGTTACTCTCTAGAG------AAAAGCAAACCCTAGCGGGACTAAA	Δ6	x6
TGTAGTGCCCCAGTTACTCTCTAGA--------AAAGCAAACCCTAGCGGGACTAAA	Δ8	x4
TGTAGTGCCCCAGTTACTCTCTAGAGC---AGAAAAGCAAACCCTAGCGGGACTAAA	Δ3	x2
TGTAGTGCCCCAG------------------------CAAACCCTAGCGGGACTAAA	Δ24	
TGTAGTGCCCCAGTTACTCTCTAGAG----------------------GGACTAAA	Δ23	
TGTAGTGCCCCAGTTACT---------------AAAGCAAACCCTAGCGGGACTAAA	Δ15	
TGTAGTGCCCCAGTTACTCTCTAG-------------CAAACCCTAGCGGGACTAAA	Δ13	
TGTAGTGCCCCAGTTACTCTCTAGAGC----------AAACCCTAGCGGGACTAAA	Δ11	
TGTAGTGCCCCAGTTACTCTCTA-----------AAGCAAACCCTAGCGGGACTAAA	Δ11	
TGTAGTGCCCCAGTTACTCTCTAGAGCTA--GAAAAGCAAACCCTAGCGGGACTAAA	Δ2	
TGTAGTGCCCCAGTTACTCTCTAGAG---------GGTAAACCCTAGCGGGACTAAA	Δ12+3	
TGTAGTGCCCCAGTTACTCTCTAGAGC----------AAAACCCTAGCGGGACTAAA	Δ11+1	
TGTAGTGCCCCAGTTACTCTCTAG------GGAAAAGCAAACCCTAGCGGGACTAAA	Δ7+1	
TGTAGTGCCCCAGTTACTCTCTAGAG---TGAAAAAGCAAACCCTAGCGGGACTAAA	Δ6+3	
TGTAGTGCCCCAGTTACTCTCTAGAGC--AAAAAAAAGCAAACCCTAGCGGGACTAAA	Δ5+3	

(B)

	TGTAGTGCCCCAGTTACTCTCTAGAGCTACAGAAAAGCAAACCCTAGCGGGACTAAA	genotype		analysis
#1	TGTAGTGCCCCAGTTACT-------GCTCTAGAAAAGCAAACCCTAGCGGGACTAAA TGTAGTGCCCCAGTTACTCTCTAGAGC----------AAACCCTAGCGGGACTAAA	Δ12+5 Δ11	out/out	
#2	TGTAGTGCCCCAGTTACT-------GCTCTAGAAAAGCAAACCCTAGCGGGACTAAA TGTAGTGCCCCAGTTACTCTCTAGAG--AGAGAAAAGCAAACCCTAGCGGGACTAAA	Δ12+5 Δ4+2	out/out	tail regression
#3	TGTAGTGCCCCAGTTACT-------GCTCTAGAAAAGCAAACCCTAGCGGGACTAAA TGTAGTGCCCCAGTTACTCTCTAGAGCTAACTAGAGAGCTAACTAGAGAAAAGCAAACCCTAGCGGGACTAAA	Δ12+5 Δ1+17	out/out	tail regression
#4	TGTAGTGCCCCAGTTACTCTCTAGAGC----------AAACCCTAGCGGGACTAAA TGTAGTGCCCCAGTTACTCTCTAGA--------AAAGCAAACCCTAGCGGGACTAAA	Δ11 Δ8	out/out	
#5	TGTAGTGCCCCAGTTACTCTCTAGAGC----------AAACCCTAGCGGGACTAAA TGTAGTGCCCCAGTTACTCTCTAGA--------AAAGCAAACCCTAGCGGGACTAAA	Δ11 Δ8	out/out	
#6	TGTAGTGCCCCAGTTACTCTCTAGAGCTA--GAAAAGCAAACCCTAGCGGGACTAAA TGTAGTGCCCCAGTTACTCTCTAGAG--AGAGAAAAGCAAACCCTAGCGGGACTAAA	Δ2 Δ4+2	out/out	
#7	TGTAGTGCCCCAGTTACTCTCTAGAGCTA--GAAAAGCAAACCCTAGCGGGACTAAA TGTAGTGCCCCAGTTACTCTCTAGA--------AAAGCAAACCCTAGCGGGACTAAA	Δ2 Δ8	out/out	tail regression
#8	TGTAGTGCCCCAGTTACTCTCTAGA--------AAAGCAAACCCTAGCGGGACTAAA TGTAGTGCCCCAGTTACTCTCTAGAG-----TAAAAGCAAACCCTAGCGGGACTAAA	Δ8 Δ6+1	out/out	
#9	TGTAGTGCCCCAGTTACTCTCTAGAGC----------AAACCCTAGCGGGACTAAA TGTAGTGCCCCAGTTACTCTCTAGA--------AAAGCAAACCCTAGCGGGACTAAA	Δ11 Δ8	out/out	tail regression
#10	TGTAGTGCCCCAGTTACTCTCTAGAGC--CAGAAAAGCAAACCCTAGCGGGACTAAA TGTAGTGCCCCAGTTACTCTCTAGA--------AAAGCAAACCCTAGCGGGACTAAA	Δ2 Δ8	out/out	qPCR Western blot
#11	TGTAGTGCCCCAGTTACTCTCTAGAGC----------AAACCCTAGCGGGACTAAA TGTAGTGCCCCAGTTACTCTCTAGA--------AAAGCAAACCCTAGCGGGACTAAA	Δ11 Δ8	out/out	tail regression

Fig. 8. Nucleotide sequences of the *ouro2* gene derived from F0 and *ouro2*-knockout F1.

(A) Mutation analysis of F0 injected with anti-*ouro2* TALEN mRNA. The target DNA fragment was amplified using pooled genomic DNA purified from ten three-day-old F0 embryos. (B) Mutation analysis of *ouro2*-knockout F1. The target DNA fragment was amplified using genomic DNA purified from the amputated tail tip of F1 obtained by mating F0 frogs. The alignment is labeled as described in the legend to Fig. 6.

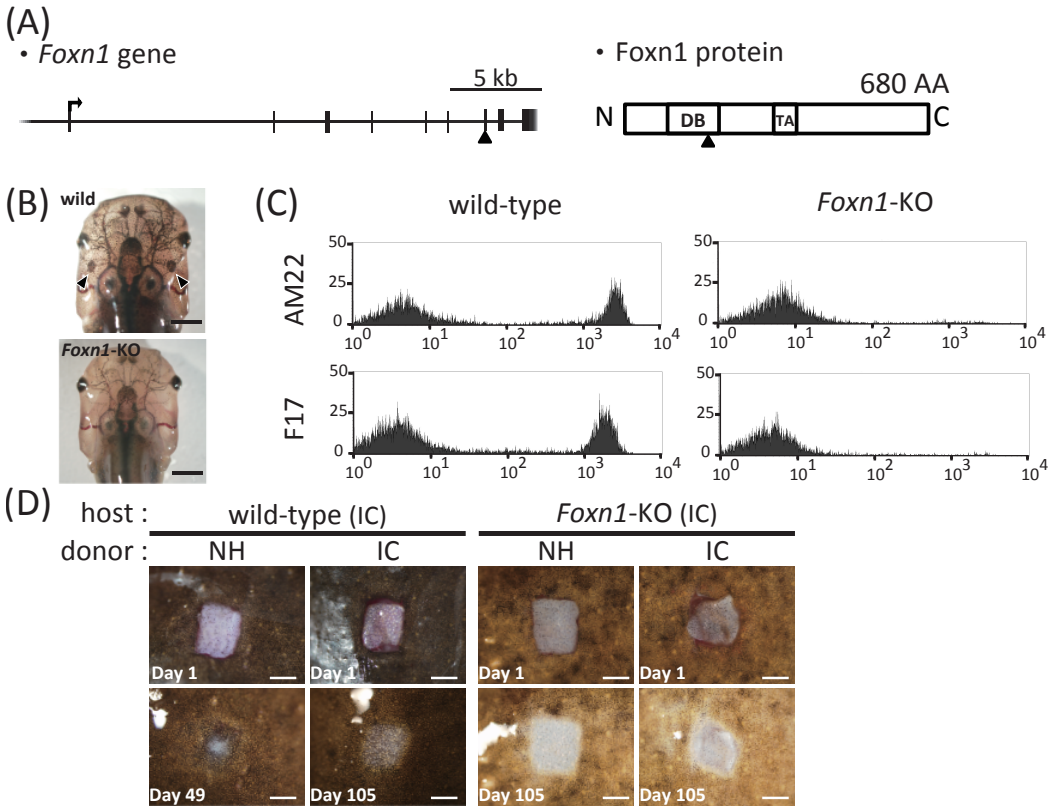

Fig. 9. Characterization of the *Foxn1*-knockout tadpoles.

(A) The target sites of anti-*Foxn1* TALEN in *Foxn1* genomic gene and Foxn1 protein. The alignment is labeled as described in the legend to Fig. 5. (B) Photographs of heads of stage 56 wild-type and *Foxn1*-knockout tadpoles. Arrowheads indicate the thymus in the wild-type tadpole. There is no thymus in the *Foxn1*-knockout tadpole. Scale bars = 3 mm. (C) Flow cytofluorometric analysis of splenocytes from wild-type and *Foxn1*-knockout frogs after staining with mouse anti-CD8 monoclonal antibody (AM22 or F17) and Alexa Fluor 488 goat anti-mouse IgM antibody. (D) Transplantation of ventral skin grafts from wild-type Nigerian H (NH) and Ivory Coast (IC) strains to the backs of IC wild-type and *Foxn1*-knockout frogs. Note that both grafts survived on the back of *Foxn1*-knockout frog for more than one hundred days. Scale bars = 1 mm.

(A)

AATCTGGAAGTTCTTCCCGTAAAGGGTGCCTGTGGGCCCTGAATCCTGCCAAGA	wild-type *Foxn1*	
AATCTGGAAGTTCTTCCCGTAAAGGG----------CCCTGAATCCTGCCAAGA	Δ10	x3
AATCTGGAAGTTCTTC------------------------AATCCTGCCAAGA	Δ25	
AATCTGGAAGTTCTTCCCGTAAAGGG---------GCCCTGAATCCTGCCAAGA	Δ9	
----------------------------------GGCCCTGAATCCTGCCAAGA	Δ62	
AATCTGGAAGTTCTTCCCGTAAAG--------TGGGCCCTGAATCCTGCCAAGA	Δ8	
AATCTGGAAGTTCTTCCCGT-------------GGGCCCTGAATCCTGCCAAGA	Δ13	
AATCTGGAAGTTCTTCCCGTAAAGGG-----AAGGGCCCTGAATCCTGCCAAGA	Δ7+2	
AATCTGGAAGTTCTTCCCGTA---------------TCCTGAATCCTGCCAAGA	Δ16+1	
AATCTGGAAGTTCTTCCC-----------TAAAGGGCCCTGAATCCTGCCAAGA	Δ15+4	
AATCTGGA----------------CAAACCTGTGGGCCCTGAATCCTGCCAAGA	Δ20+4	

(B)

	AATCTGGAAGTTCTTCCCGTAAAGGGTGCCTGTGGGCCCTGAATCCTGCCAAGA	genotype		analysis
#1	AATCTGGAAGTTCTTCCCGTAA----------GGGGCCCTGAATCCTGCCAAGA	Δ11+1	out/out	tail regression transplantation
	AATCTGGAAGTTCTTCC-------------TGTGGGCCCTGAATCCTGCCAAGA	Δ13		
#2	AATCTGGAAGTTCTTCCCGTAA----------GGGGCCCTGAATCCTGCCAAGA	Δ11+1	out/out	tail regression transplantation
	AATCTGGAAGTTCTTCCC-----------CTGTGGGCCCTGAATCCTGCCAAGA	Δ11		
#3	AATCTGGAAGTTCTTCCCGTAAAGGG--------GGCCCTGAATCCTGCCAAGA	Δ8	out/out	tail regression transplantation
	AATCTGGAAGTTCTTCCCGT-----------GTGGGCCCTGAATCCTGCCAAGA	Δ11		
#4	AATCTGGAAGTTCTTCC-------------TGTGGGCCCTGAATCCTGCCAAGA	Δ13	out/out	transplantation
	AATCTGGAAGTTCTTCCCGT-----------GTGGGCCCTGAATCCTGCCAAGA	Δ11		
#5	AATCTGGAAGTTCTTCCC-----------CTGTGGGCCCTGAATCCTGCCAAGA	Δ11	out/out	tail regression
	AATCTGGAAGTTCTTCCCGT-----------GTGGGCCCTGAATCCTGCCAAGA	Δ11		
#6	AATCTGGAAGTTCTTCC-------------TGTGGGCCCTGAATCCTGCCAAGA	Δ13	out/out	tail regression transplantation
	AATCTGGAAGTTCTTCCCGT-----------GTGGGCCCTGAATCCTGCCAAGA	Δ11		
#7	AATCTGGAAGTTCTTCC-------------TGTGGGCCCTGAATCCTGCCAAGA	Δ13	out/out	tail regression
	AATCTGGAAGTTCTTCCCGT-----------GTGGGCCCTGAATTCTGCCAAGA	Δ11		
#8	AATCTGGAAGTTCTTCCCGTAA----------GGGGCCCTGAATCCTGCCAAGA	Δ11+1	out/out	tail regression
	AATCTGGAAGTTCTTCC-------------TGTGGGCCCTGAATCCTGCCAAGA	Δ13		
#9	AATCTGGAAGTTCTTCC-------------TGTGGGCCCTGAATCCTGCCAAGA	Δ13	out/out	tail regression
	AATCTGGAAGTTCTTCCCGT-----------GTGGGCCCTGAATCCTGCCAAGA	Δ11		
#10	AATCTGGAAGTTCTTCCCGTAA----------GGGGCCCTGAATCCTGCCAAGA	Δ11+1	out/out	tail regression
	AATCTGGAAGTTCTTCCC-----------CTGTGGGCCCTGAATCCTGCCAAGA	Δ11		
#11	AATCTGGAAGTTCTTCC-------------TGTGGGCCCTGAATCCTGCCAAGA	Δ13	out/out	
	AATCTGGAAGTTCTTCCCGTAA----------GGGGCCCTGAATCCTGCCAAGA	Δ11+1		
#12	AATCTGGAAGTTCTTCC-------------TGTGGGCCCTGAATCCTGCCAAGA	Δ13	out/out	
	AATCTGGAAGTTCTTCCCGT-----------GTGGGCCCTGAATCCTGCCAAGA	Δ11		
#13	AATCTGGAAGTTCTTCCCGTAA-------------GCCCTGAATCCTGCCAAGA	Δ13	out/out	flow cytometry
	AATCTGGAAGTTCTTCCCGTAA----------GGGGCCCTGAATCCTGCCAAGA	Δ11+1		
#14	AATCTGGAAGTTCTTCCCGTAA----------GGGGCCCTGAATCCTGCCAAGA	Δ11+1	out/out	
	AATCTGGAAGTTCTTCCC-----------CTGTGGGCCCTGAATCCTGCCAAGA	Δ11		

Fig. 10. Nucleotide sequences of the *Foxn1* gene derived from F0 and *Foxn1*-knockout F1.

(A) Mutation analysis of F0 injected with anti-*Foxn1* TALEN mRNA. The target DNA fragment was amplified using pooled genomic DNA purified from ten three-day-old F0 embryos. (B) Mutation analysis of *Foxn1*-knockout F1. The target DNA fragment was amplified using genomic DNA purified from the amputated tail tip of F1 obtained by mating F0 frogs. The alignment is labeled as described in the legend to Fig. 6.

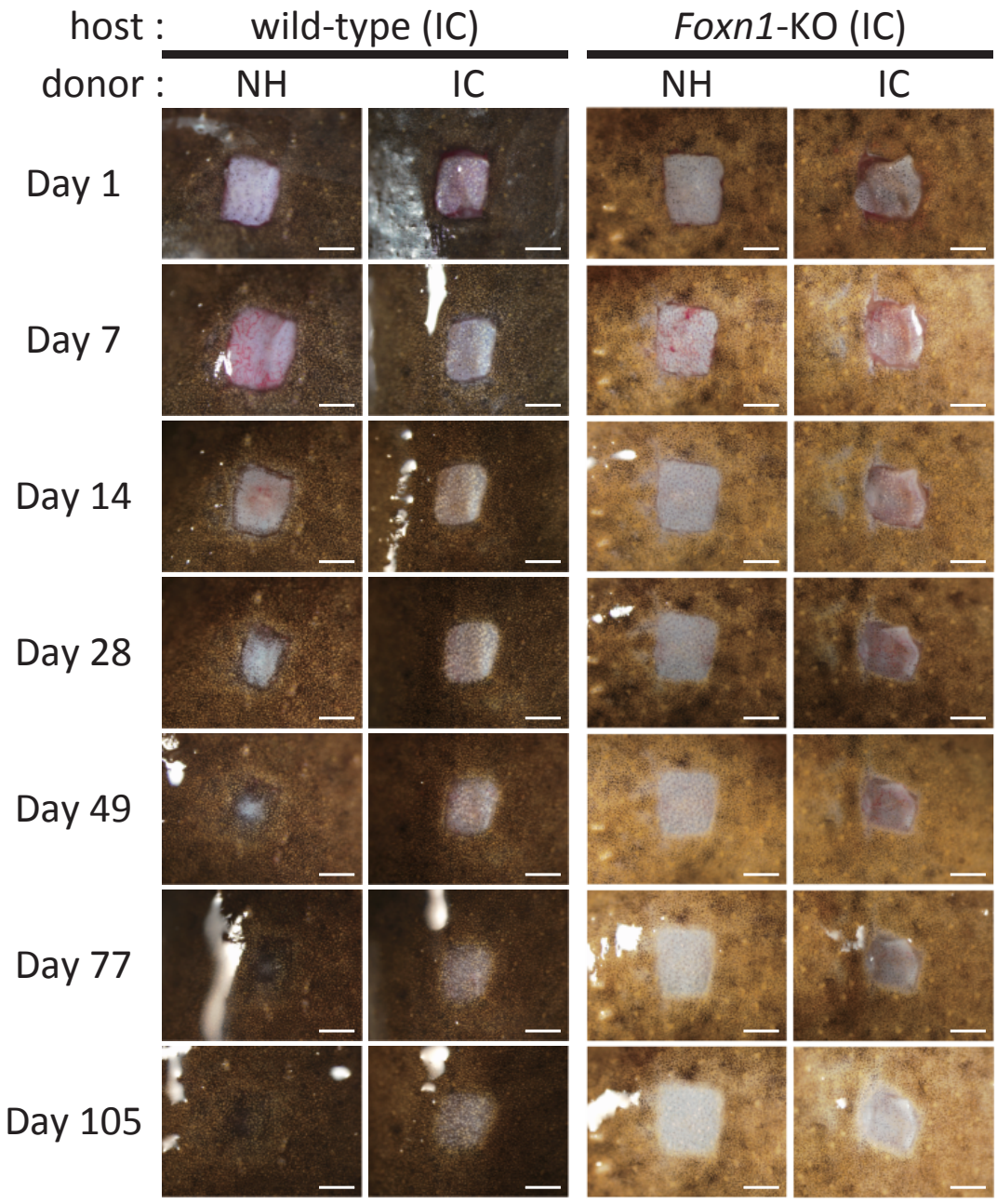

Fig. 11. Transplantation of ventral skin grafts from wild-type Nigerian H (NH) and Ivory Coast (IC) strains to the backs of IC wild-type and *FoxnI*-knockout frogs. Note that skin grafts from the NH and IC strains were rejected by the wild-type IC strain rapidly and slowly, respectively, and both grafts were accepted on the backs of *Foxn1*-knockout frogs for more than one hundred days. Scale bars = 1 mm.

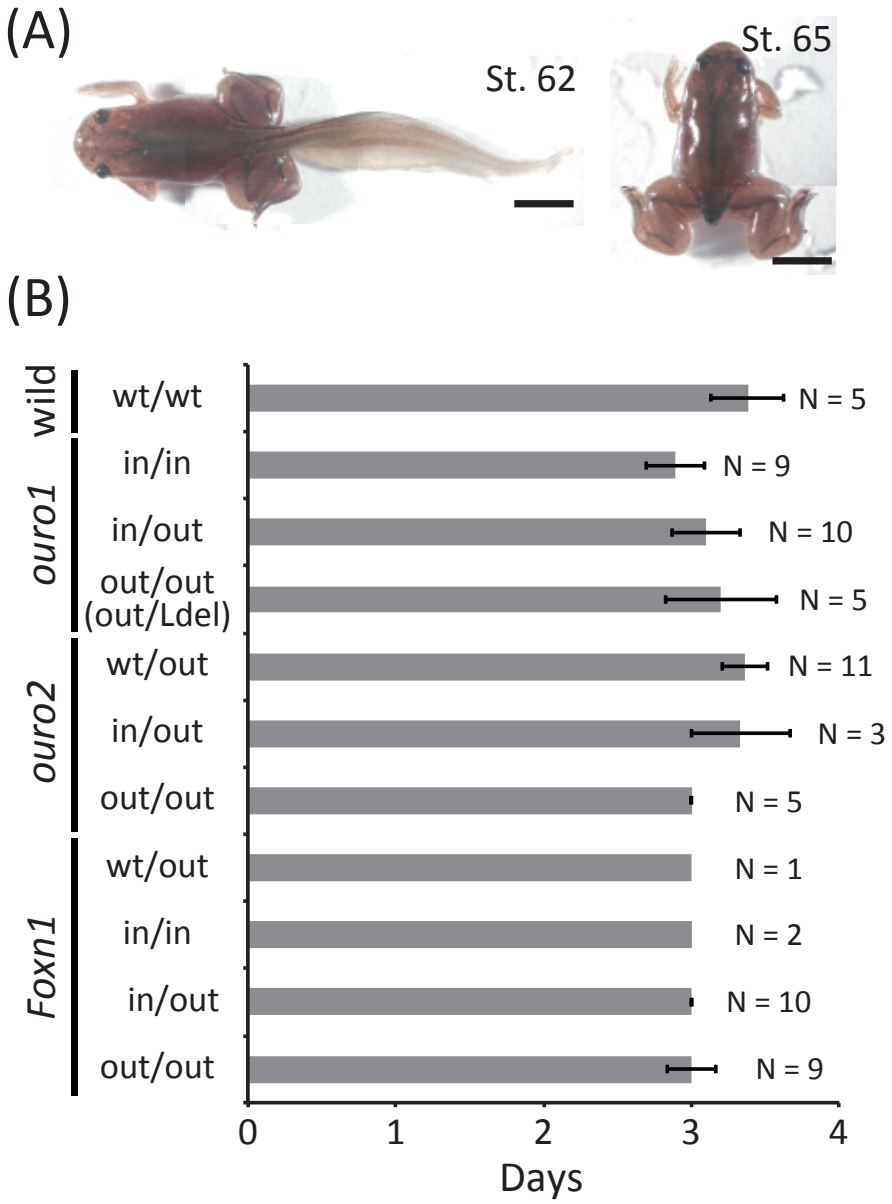

Fig. 12. Tails regressed in *ouro1*-, *ouro2*-, and *Foxn1*-knockout tadpoles similarly to wild-type tadpoles.

(A) Photographs of wild-type stage 62 and 65 tadpoles. Scale bars = 5 mm. (B) The time required for wild-type tadpoles and *ouro1*-, *ouro2*-, and *Foxn1*-knockout tadpoles to develop from stage 62 to 65. Data are expressed as the means ± s.e.m. wt, wild-type; in, in-frame mutation; out, out-of-frame mutation; Ldel, a large deletion.

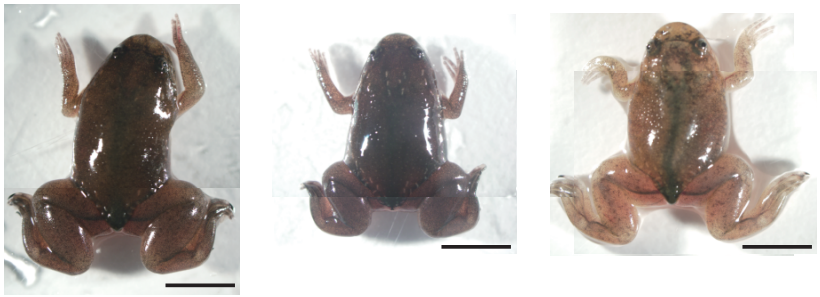

Fig. 13. *ouro1*-, *ouro2*-, and *Foxn1*-knockout froglets just after metamorphosis. Scale bars = 5 mm.

Table 1. Nucleotide sequences of primers used in this study

primer name	sequence	Purpose
ouro1-F1	5'-GGCAGAAGTGCTAGGGCTGG-3'	mutation analysis of F0
ouro1-R1	5'-CTATGTGTCCTGGTACAAGTG-3'	mutation analysis of F0
ouro1-F2	5'-TAGATTAGGGGGCGCTTTTGGTGT-3'	mutation analysis of F1
ouro1-R2	5'-CCCCTTTGGGACTGGATGCC-3'	mutation analysis of F1
ouro1-F3	5'-CTGCTAGGAGTTTGTTGGCATTCC-3'	mutation analysis of F1 (large deletion)
ouro1-R3	5'-CAACCATGGCTACTCTCAGTCAGA-3'	mutation analysis of F1 (large deletion)
ouro2-F1	5'-CATGGTGCAGCTTCTGGTGGT-3'	mutation analysis of F0
ouro2-R1	5'-AGCTCTTCAGCTGCTCCTC-3'	mutation analysis of F0
ouro2-F2	5'-TTGGTGGAGGTTTAGGAGGAAGTG-3'	mutation analysis of F1
ouro2-R2	5'-GATGTAACAGAAGTGCCACCTGTC-3'	mutation analysis of F1
Foxn1-F1	5'-AGTCCTGGGGCCTATCAAACAGAG-3'	mutation analysis of F0
Foxn1-R1	5'-GGGCCAGTCTGACACTGGGTAGAA-3'	mutation analysis of F0
Foxn1-F2	5'-TTGTTGGGTAGCAGCATGCAACAC-3'	mutation analysis of F1
Foxn1-R2	5'-TGAGGCCCTTGGTTTGGGTGTATT-3'	mutation analysis of F1
ouro1-RTF3'	5'-GTCATCAGTCCAAGCCCTGACATC-3'	qPCR for *ouro1* mRNA (3')
ouro1-RTR3'	5'-CGCGGCTTGCTCCTGATATGTATC-3'	qPCR for *ouro1* mRNA (3')
ouro1-RTF5'	5'-ATGACTGAGAAGCAAGTGAAAGT-3'	qPCR for *ouro1* mRNA (5')
ouro1-RTR5'	5'-CCTCCATAGGATGCGCCATA-3'	qPCR for *ouro1* mRNA (5')
ouro2-RTF3'	5'-CTGCTACTGAATTGCGCACCATAC-3'	qPCR for *ouro2* mRNA (3')
ouro2-RTR3'	5'-TGCAGCACCCAGCTTGCTTTGTAG-3'	qPCR for *ouro2* mRNA (3')
ouro2-RTF5'	5'-ATCTGGATACTCGCTTGCACATGG-3'	qPCR for *ouro2* mRNA (5')
ouro2-RTR5'	5'-AACCACTACCCAAACCAAGACCAG-3'	qPCR for *ouro2* mRNA (5')
EF1a-RTF	5'-CCTCCATAGGATGCGCCATA-3'	qPCR for *EF1α* mRNA
EF1a-RTR	5'-AAGGACACCAGTCTCCACAC-3'	qPCR for *EF1α* mRNA
ouro1-BamHI	5'-GGGGGATCCACGATGGTTGCCACCACTGCTGTTGCTGGT-3'	cloning of ouro1gene
ouro1-EcoRI	5'-GGGGAATTCGCAGATGGGGAGACTTTACAGCTC-3'	cloning of ouro1gene
ouro2-BamHI	5'-GGGGGATCCATCATGTCCATCTCAGGCTCAAG-3'	cloning of ouro2gene
ouro2-EcoRI	5'-GGGGAATTCTTAGTGTAATTCTGTGCTTGATTCC-3'	cloning of ouro2gene
T3-pCMV	5'-CGAAATTAACCCTCACTAAAGGGAGGTCTATATAAGCAGAG-3'	mRNA synthesis
mCherry-pT	5'-TTTTTTTTTTTTTTTTTTTTTTTTTTTTTGGACAAACCACAACTAGAATG-3'	mRNA synthesis
pCMV-3'pT	5'-TTTTTTTTTTTTTTTTTTTTTTTTTTTTTTTTGGGTACACTTACCTGG-3'	mRNA synthesis

Table 2. Result of search for ortholog of *ouro* genes.

DNA

Query sequence	Result	Identity
X.laevis ouro1	*X.tropicalis ouro1*	1630/1846(88 %)
	keratin, type I cytoskeletal 47 kDa-like, transcript variant X1	194/252 (77 %)
	X.tropicalis ouro2	126/169 (75 %)
X.laevis ouro2	*X.tropicalis ouro2*	1359/1474 (92 %)
	keratin-3, type I cytoskeletal 51 kDa-like	131/181 (72 %)
	keratin 5, type II	155/200 (78 %)

Protein

Query sequence	Result	Identity
X.laevis Ouro1	*X.tropicalis* Ouro1	90%
	Ina_protein_partial	25%
	Krt5.7 protein, partial	33%
X.laevis Ouro2	*X.tropicalis* Ouro2	91%
	Keratin, type I cytoskeletal 19-like	33%

The homology search by BLAST was performed using *X.laevis ouro* gene sequences for *X.tropicalis* genome database. Only one gene locus was found as *ouro1* and *ouro2* orthologs, respectively. In the case that the query sequence was *X.laevis ouro1* or *ouro2* nucleotide sequence, the homologous regions were only short sequences except for the corresponding ortholog of *X.tropicalis*. In the case that the query sequence was *X.laevis* Ouro1 or Ouor2 amino acid sequence, the most similar protein was the corresponding ortholog.

Table 3. Genotype analysis of F1 tadpoles

	genotype							
	wt/wt	wt/in	wt/out	in/in	in/out	out/out	in/Ldel	out/Ldel
ouro1	0	0	0	24	20	5	7	2
	(0.0%)	(0.0%)	(0.0%)	(43.6%)	(36.4%)	(9.1%)	(12.7%)	(3.6%)
ouro2	2	3	25	0	6	11	0	0
	(4.3%)	(6.4%)	(53.2%)	(0.0%)	(12.8%)	(23.4%)	(0.0%)	(0.0%)
Foxn1	0	0	1	2	10	14	0	0
	(0.0%)	(0.0%)	(3.7%)	(7.4%)	(37.0%)	(51.9%)	(0.0%)	(0.0%)

Only athymic tadpoles were selected in F1 offspring obtained by mating F0 frogs that had been injected by anti-*Foxn1* TALEN mRNA. wt, wild-type target sequence; in, in-frame mutation; out, out-of-frame mutation; Ldel, a large deletion of 715 bp containing the initiation codon.

公表論文

Ouro proteins are not essential to tail regression during *Xenopus tropicalis* metamorphosis.

Yuya Nakai, Keisuke Nakajima, Jacques Robert and Yoshio Yaoita

to be published in ***Gene to Cells***.

参考論文

Targeted gene disruption in the *Xenopus tropicalis* genome using designed TALE nucleases

Keisuke Nakajima, Yuya Nakai, Morihiro Okada and Yoshio Yaoita

Zoological Science 30(6):455-460. 2013